

Universal scaling law for energy and pressure in a shearing fluid

Caroline Desgranges and Jerome Delhommelle

Department of Chemistry, University of North Dakota, Grand Forks, North Dakota 58201, USA

(Received 18 February 2009; published 14 May 2009)

Using nonequilibrium molecular-dynamics simulation, we study the shear-rate dependence of pressure and potential energy in a liquid metal subjected to shear. We show that both thermodynamic properties vary according to a power law $\dot{\gamma}^\beta$ of the shear rate $\dot{\gamma}$, in which the exponent β is a simple linear function of temperature and density. Moreover, we establish that the coefficients for this linear law are the same as those previously obtained for a Lennard-Jones fluid by Ge *et al.* [Phys. Rev. E **67**, 061201 (2003)]. This is a strong indication that these coefficients, as well as the linear law for β , could be applicable to any atomic fluid. It is also an important step toward the determination of a nonequilibrium equation of state, which would predict the value of pressure and energy of a shearing fluid for any state point and any value of the applied shear rate.

DOI: [10.1103/PhysRevE.79.052201](https://doi.org/10.1103/PhysRevE.79.052201)

PACS number(s): 61.20.Ja, 66.20.-d, 82.20.Wt, 83.50.Ax

The properties of liquids subjected to shear are of great significance from both a technological and fundamental standpoint. In recent years, nonequilibrium molecular-dynamics (NEMD) simulation methods have emerged as an important tool to study these systems [1]. However, despite the progress in the field, many issues have yet to be addressed. For instance, the exact dependence on the applied shear rate $\dot{\gamma}$ of the pressure and the energy of shearing fluids, modeled with realistic many-body potentials, remains an unsolved issue. Early NEMD studies on simple fluids, modeled with a pair potential such as, e.g., the Lennard-Jones (LJ) or the Weeks-Chandler-Anderson potentials, have concluded that pressure exhibited a shear-rate dependence of $\dot{\gamma}^{3/2}$, in agreement with the predictions of mode-coupling theory (MCT) [2]. More recently, Matin *et al.* [3] suggested that the $\dot{\gamma}^{3/2}$ variation in pressure and energy as a function of shear was only observed in the vicinity of the triple point. Subsequently, Ge *et al.* [4,5] carried out simulations on a LJ fluid and found that pressure and energy exhibited both a shear-rate dependence of $\dot{\gamma}^\beta$, in which β is a linear function of the density and of the temperature. It remains to be seen whether their conclusions only hold for the LJ system or if they may be applicable to fluids, modeled with a realistic many-body potential.

Because of the computational cost associated with realistic many-body potentials, there have been few studies on nonequilibrium systems modeled with such potentials [6]. Two studies, by Lee *et al.* [7] and by Marcelli *et al.* [8], were devoted to systems of rare gases under shear, modeled with a Barker-Fisher-Watts two-body potential, supplemented by a three-body Axilrod-Teller potential. The study by Lee *et al.* [7] tended to indicate a $\dot{\gamma}^{3/2}$ dependence for both pressure and energy, while Marcelli *et al.* [8] pointed toward a $\dot{\gamma}^2$ dependence for both properties. In recent work [9], we studied the rheology of five liquid metals, modeled with a many-body embedded atom model. We showed that, at the melting point at $P=1$ atm, all the liquid metals considered in Ref. [9] exhibited the same shear-rate dependence for pressure (with an exponent of ~ 1.2) and for the various contributions to the potential energy (with exponents varying from ~ 1 to ~ 1.2). To our knowledge, no systematic study, over a wide range of temperature and densities, of the shear-rate depen-

dence of the thermodynamic properties of shearing fluids has been carried out for systems modeled with many-body potentials. In this work, we simulate 20 state points for a system of liquid Pb, modeled with a many-body potential and subjected to shear flow. For each state point, we determine the exponents characterizing the dependence of pressure and energy upon the applied shear rate $\dot{\gamma}$. The goal of this work is threefold: (i) to determine whether pressure and potential energy exhibit the same shear-rate dependence, (ii) to find the simplest yet accurate relation between the exponents and density and temperature, and (iii) to find out if the linear law obtained for a LJ fluid [5] also holds for a liquid metal such as Pb.

We model the Pb atoms with the quantum-corrected Sutton-Chen potential [10]. The potential energy U_{total} of a system of N atoms is given by

$$U_{\text{total}} = U_{\text{two-body}} + U_{\text{many-body}} \\ = \frac{1}{2} \sum_{i=1}^N \sum_{j \neq i} \varepsilon \left(\frac{a}{r_{ij}} \right)^n - \varepsilon C \sum_{i=1}^N \sqrt{\rho_i} \quad (1)$$

in which r_{ij} is the distance between two atoms i and j and the density term ρ_i is given by $\rho_i = \sum_{j \neq i} \left(\frac{a}{r_{ij}} \right)^m$. We use the set of parameters proposed by Luo *et al.* [10]: $a=4.9495$ Å, $\varepsilon=0.55772 \times 10^{-2}$ eV, $C=45.882$, $m=7$, and $n=10$. This model accurately describes both the thermodynamic and the transport properties of Pb and other metals [9–12].

We use the Sllod equations of motion [1] to simulate liquid Pb undergoing shear flow,

$$\dot{\mathbf{r}}_i = \frac{\mathbf{p}_i}{m} + \dot{\gamma} y_i \mathbf{e}_x, \\ \dot{\mathbf{p}}_i = \mathbf{F}_i - \dot{\gamma} p_{y_i} \mathbf{e}_x - \alpha \mathbf{p}_i, \\ \alpha = \frac{\sum_{i=1}^N \mathbf{p}_i \cdot \mathbf{F}_i / m_i}{\sum_{i=1}^N \mathbf{p}_i^2 / m_i}. \quad (2)$$

In Eq. (2), \mathbf{r}_i , \mathbf{p}_i , and m denote the position, momentum, and mass of particle i , \mathbf{F}_i is the force exerted on particle i , N is the number of particles, \mathbf{e}_x is a unit vector along the x axis, $\dot{\gamma}$

is the applied shear rate, and α is the Gaussian thermostat multiplier [1]. The choice of a thermostat may have a significant effect on the results under far-from-equilibrium conditions [13–18], for shear rates typically larger than 10^{12} s^{-1} [19,20]. In this work, we restrict our study to shear rates lower than 10^{12} s^{-1} .

We integrate the equations of motion for systems of 512 Pb atoms with the operator splitting algorithm presented in Ref. [21] and a time step of 10 fs. We study 20 different state points. We start from a liquid of Pb at the melting point at ambient pressure, i.e., at a density of $d_m = 9.79 \text{ g cm}^{-3}$ and $T_m = 575 \text{ K}$. In the rest of this work, we reduce the temperature with respect to the melting temperature, $T^* = T/T_m$, and the density with respect to the density at the melting point, $d^* = d/d_m$. We then carry out simulations for 19 other state points for temperatures ranging from $T^* = 1$ up to $T^* = 1.5$ and for densities ranging from $d^* = 1$ down to $d^* = 0.85$. All state points studied in this work lie in the dense fluid region of the phase diagram of Pb. For each state point, we first carry out a 20 ns equilibrium molecular-dynamics run during which we calculate the shear viscosity according to the Green-Kubo formalism

$$\eta = \frac{V}{k_B T} \int_0^\infty \langle P_{xy}(s) P_{xy}(0) \rangle ds, \quad (3)$$

in which P_{xy} is the shear stress [6]. We also evaluate the average of the square of the shear stress to determine the infinite frequency shear modulus according to $G_\infty = V \langle P_{xy}^2(0) \rangle / k_B T$ and the Maxwell relaxation time as $\tau_M = \eta / G_\infty$. Then, for each state point, we carry out nonequilibrium molecular-dynamics simulations with the equations of motion presented in Eq. (2) for ten different shear rates ranging from 10^{10} s^{-1} to 10^{12} s^{-1} . This range of shear rates allows us to access both the Newtonian regime and the non-Newtonian regime. Additional calculations were also carried out on a few state points for very low shear rates (down to 10 s^{-1}), using a combination of NEMD simulations with the transient-time correlation function formalism (TTCF) method (see Refs. [9,12] for more details). The TTCF results were in excellent agreement with the NEMD results, obtained for higher shear rates, thereby confirming that the range of shear rates studied in the NEMD simulations provides an accurate picture of the shear-rate dependence of pressure and energy. For each shear rate, we first carry out a run of 0.5 ns to allow the system to reach a steady state and then a second run of 1 ns, over which we collect the averages of the pressure $P(\dot{\gamma})$, of the two-body contribution to the potential energy $U_{\text{two-body}}(\dot{\gamma})$, of the many-body contribution to the potential energy $U_{\text{many-body}}(\dot{\gamma})$, and of the total potential energy $U_{\text{total}}(\dot{\gamma})$. We then rescale [9] the shear rate $\dot{\gamma}$ by the inverse of τ_M , the average of pressure by G_∞ , and the averages for all contributions to the potential energy by their average value at equilibrium (collected during the 20 ns equilibrium molecular-dynamics run). We then fit the following power-law forms to the simulations results for the pressure $P(\dot{\gamma}\tau_M)$:

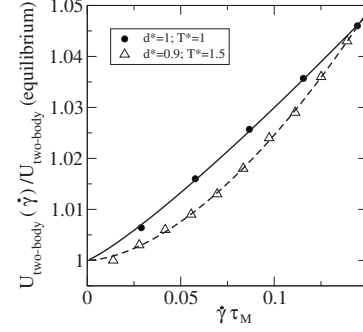


FIG. 1. Variation in $U_{\text{two-body}}(\dot{\gamma})/U_{\text{two-body, equilibrium}}$ as a function of $\dot{\gamma}$, $U_{\text{two-body}}(\dot{\gamma})$. Results are shown for two state points: filled circles (●) are results obtained for ($d^* = 1$, $T^* = 1$) while open triangles (△) are for ($d^* = 0.9$, $T^* = 1.5$).

$$\frac{P(\dot{\gamma}\tau_M) - P_{\text{equilibrium}}}{G_\infty} = A_P (\dot{\gamma}\tau_M)^{\beta_P}, \quad (4)$$

where $P(\dot{\gamma}\tau_M)$ is the trace of the pressure tensor. The elements of the pressure tensor are evaluated according to the formalism proposed by Stankovic *et al.* [6]. Similarly, we perform the following fit for $U(\dot{\gamma}\tau_M)$:

$$\frac{U_{\text{total}}(\dot{\gamma}\tau_M)}{U_{\text{total, equilibrium}}} = 1 + A_{U_{\text{total}}} (\dot{\gamma}\tau_M)^{\beta_{U_{\text{total}}}}, \quad (5)$$

for $U_{\text{two-body}}(\dot{\gamma}\tau_M)$,

$$\frac{U_{\text{two-body}}(\dot{\gamma}\tau_M)}{U_{\text{two-body, equilibrium}}} = 1 + A_{U_{\text{two-body}}} (\dot{\gamma}\tau_M)^{\beta_{U_{\text{two-body}}}}, \quad (6)$$

and for $U_{\text{many-body}}(\dot{\gamma}\tau_M)$,

$$\frac{U_{\text{many-body}}(\dot{\gamma}\tau_M)}{U_{\text{many-body, equilibrium}}} = 1 + A_{U_{\text{many-body}}} (\dot{\gamma}\tau_M)^{\beta_{U_{\text{many-body}}}}. \quad (7)$$

We first discuss the variations for the power-law exponents for each property as a function of the state point studied. As an example, we provide in Fig. 1 the NEMD results obtained for the two-body contribution to the potential energy for two state points, ($d^* = 1$, $T^* = 1$) and ($d^* = 0.9$, $T^* = 1.5$), together with the power-law fits obtained with Eqs. (4)–(7). We find an exponent $\beta_{U_{\text{two-body}}} = 1.17$ for the first state point and an exponent $\beta_{U_{\text{two-body}}} = 1.70$ for the second state point. We obtained similar results for all four properties (P , U_{total} , $U_{\text{two-body}}$, and $U_{\text{many-body}}$) studied in this work. We draw four main conclusions from these results. First, we find the value of the exponents to be state-point dependent for all properties. Second, the exponents vary between ~ 1.1 and ~ 2 for all properties. Third, the $\dot{\gamma}^{3/2}$ dependence predicted by MCT only holds for a very small region of the phase diagram. Fourth, when we compare the values taken by various exponents β_P , $\beta_{U_{\text{total}}}$, $\beta_{U_{\text{two-body}}}$, and $\beta_{U_{\text{many-body}}}$ for a given state point, we find that all exponents are always within less than 5% of each other. This demonstrates that the thermodynamic properties of liquid Pb under shear are accurately described by a single power law of the shear rate $\dot{\gamma}^\beta$, in which β is the same for all properties. These four points establish that the thermodynamic properties of a

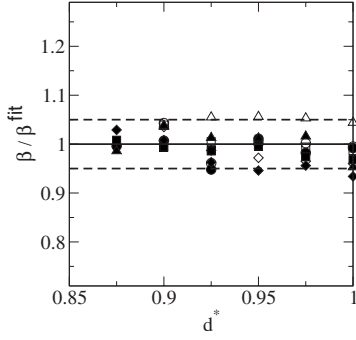


FIG. 2. Ratio between β , determined from the simulations, and β_{fit} , predicted by Eq. (8), as a function of d^* . The solid line indicates a perfect correspondence between β and β_{fit} . The dashed line delimits the zone in which there is less than 5% of difference between β and β_{fit} . Results are presented for P (\circ), $U_{\text{two-body}}$ (\square), $U_{\text{many-body}}$ (\diamond), and U_{total} (\triangle). Filled symbols are obtained for $T^*=1.2$ while open symbols are for $T^*=1.5$.

liquid metal undergoing shear flow are *at the very least* qualitatively the same as those of a shearing LJ liquid [5].

We now quantify the state-point dependence of β and set on to find the simplest, yet accurate, relation between β , d^* , and T^* . We rapidly find that a simple linear scaling law of the temperature and density allows us to accurately reproduce the exponents obtained from the NEMD results. The linear scaling law we obtain is given by the following equation:

$$\begin{aligned} \beta &= a_0 + a_1 T^* - a_2 d^* \\ &= (3.7 \pm 0.04) + (0.44 \pm 0.04) T^* - (2.95 \pm 0.04) d^*. \end{aligned} \quad (8)$$

This simple linear scaling law reproduces the results obtained for the 20 state points with a relative root-mean-square error of 0.047. To give a better sense of the accuracy of the fitting procedure, we compute the ratio of the exponents estimated from the NEMD simulations to the value predicted by the linear scaling law. We present in Fig. 2 the results obtained for two temperatures $T^*=1.2$ and $T^*=1.5$. For all state points, we find the ratio to be very close to 1 for all four properties. This means that the NEMD results are all in good agreement, and always within at most $\sim 5\%$, with the value given by Eq. (8). We also find that for all properties, the exponent is neither systematically underestimated nor systematically overestimated by the linear scaling law. This fit also means that if we plot the variations in the exponent β given by Eq. (8) as a function of temperature and density, we obtain a plane in the thermodynamic state space. The predictions from MCT (i.e., states for which $\beta=3/2$) are recovered for state points at the intersection between the two planes of equations $\beta=3/2$ and Eq. (8). As observed for the LJ fluid, β is close to $3/2$ for only a small region of the thermodynamic state space. For liquid Pb, we find that this region corresponds to a line of equation

$$(2.95 \pm 0.04) d^* - (0.44 \pm 0.04) T^* = (2.2 \pm 0.04). \quad (9)$$

In previous work [9], we showed that the thermodynamic properties of several fcc metals exhibited the same shear-rate

dependence at the melting point. We also found that for four different state points, the shear stress autocorrelation function as a function of time could be superimposed onto one another for all these metals. These two facts are a strong indication that Eq. (8) can be used to reliably predict the value of the exponent β for any state point and any metal. This means that using this value for β together with the power laws of Eqs. (4)–(7), we can predict the value taken by pressure and energy of a liquid metal undergoing shear flow for any value of the applied shear rate. In other words, these equations constitute a set of nonequilibrium equation of states for the properties of liquid metals subjected to shear.

We now attempt to make a connection between the results obtained for Pb and the results obtained on the LJ fluid by Ge *et al.* [5]. For this purpose, we need to write the scaling laws, obtained in this work for Pb and for the LJ fluid [5]. We, therefore, consider the two systems at an equivalent state point, e.g., the melting point at zero pressure. The scaling law we obtain for Pb is written in the following system of reduced units: the temperature and the mass density are reduced with respect to the melting temperature and densities at zero pressure. We now re-write this scaling law in terms of the reduced number density $\rho^* = N/V^{*3}$, where V^* is the reduced volume, rather than the reduced mass density d^* . Using the unit length we introduced for Pb ($2 \times r_{\text{Pb}}$), we have $\rho^* = 8r_{\text{Pb}}^3 \rho$ where ρ is the number density. We then obtain for the reduced mass density $d^* = M/[9.79N_A(8r_{\text{Pb}}^3)] \times \rho^*$, where $M=207.2$ g mol $^{-1}$ is the atomic weight for Pb and N_A the Avogadro number. If we plug the expression of d^* as a function of ρ^* in Eq. (8), we obtain the following scaling law:

$$\begin{aligned} \beta &= a_0 + a_1 T^* - \frac{Ma_2}{8r_{\text{Pb}}^3 \times 9.79N_A} \rho^* \\ &= (3.7 \pm 0.04) + (0.44 \pm 0.04) T^* - (2.42 \pm 0.03) \rho^*. \end{aligned} \quad (10)$$

We now turn to the scaling law proposed by Ge *et al.* for the LJ fluid [5],

$$\beta = A + BT^* - C\rho^*, \quad (11)$$

where T^* is the reduced temperature, $T^* = k_B T / \varepsilon$, and ρ^* is the reduced number density, $\rho^* = \rho \sigma^3 = (N/V) \sigma^3$. With this set of reduced units, Ge *et al.* obtained the following parameters: $A = 3.67 \pm 0.04$, $B = 0.69 \pm 0.03$, and $C = 3.35 \pm 0.03$. Instead of rescaling the temperature by ε/k_B , we use the melting temperature of the LJ fluid at zero pressure and rescale the temperature by $0.69\varepsilon/k_B$ [22]. Then, instead of using σ as the unit length, we use the equilibrium distance between two LJ particles, $2^{1/6}\sigma$. This means that we need to multiply the number density ρ by $\sqrt{2}\sigma^3$ instead of σ^3 to obtain the reduced number density ρ^* . With this new set of reduced units, we obtain the following law for the fit proposed by Ge *et al.*:

$$\begin{aligned} \beta &= A + 0.69 \times BT^* - \frac{C}{\sqrt{2}} \rho^* \\ &= (3.67 \pm 0.04) + (0.48 \pm 0.02) T^* - (2.37 \pm 0.02) \rho^*. \end{aligned} \quad (12)$$

The parameters obtained for liquid Pb [Eq. (10)] and for the LJ fluid [Eq. (12)] are in excellent agreement with each other. This finding has two very significant consequences. First, since the same linear law, with the same coefficients, can be used to quantify the shear-rate dependence of the exponent β for fluids modeled with very different interaction potentials, this result constitutes an evidence of the universality of the linear law for β for all atomic fluids. Second, this finding is an important step toward the determination of a nonequilibrium equation of state for all atomic fluids. Since the exponent β can be estimated from Eq. (10) for any atomic fluid and any state point, the value taken by the pressure and the potential energy (including all components such as, e.g., the two-body as well as the many-body contributions in the case of Pb) can be calculated for any shear rate using Eqs. (4)–(7).

Some questions are still unanswered. For instance, does a similar universal scaling exist for the shear viscosity? Todd [23] showed that for the LJ fluid, the shear viscosity varies according to a power law of the shear rate with an exponent,

whose value is a linear function of density and temperature. To determine if the same relation holds for liquid Pb, we fitted our results for the shear viscosity with a power law with an exponent β_η . We found that β_η varied from ~ 0.5 to ~ 1.4 and increased with either an increase in temperature or a decrease in density. β_η was in agreement with the predictions from MCT (~ 0.5) over a very narrow region of the thermodynamic state space. However, attempts to fit β_η with a linear law of density and temperature were deemed to be inconclusive. Our results, together with the findings of Ge *et al.* [5], shed light on some of the limitations of MCT [2]. We hope these results will prompt liquid state theorists to improve on this theory to account for the universal state-point dependence of the exponent β observed for atomic fluids.

Acknowledgment is made to the Donors of the American Chemical Society Petroleum Research Fund, for partial support of this research and to the UND Computational Research Center for a substantial allocation of time on the linux beowulf cluster.

-
- [1] D. J. Evans and G. P. Morriss, *Statistical Mechanics of Non-equilibrium Liquids* (Academic Press, London, 1990).
- [2] K. Kawasaki and J. D. Gunton, *Phys. Rev. A* **8**, 2048 (1973).
- [3] M. Matin, P. J. Daivis, and B. D. Todd, *J. Chem. Phys.* **113**, 9122 (2000).
- [4] J. Ge, G. Marcelli, B. D. Todd, and R. J. Sadus, *Phys. Rev. E* **64**, 021201 (2001).
- [5] J. Ge, B. D. Todd, G. Wu, and R. J. Sadus, *Phys. Rev. E* **67**, 061201 (2003).
- [6] I. Stankovic, S. Hess, and M. Kroger, *Phys. Rev. E* **69**, 021509 (2004).
- [7] S. H. Lee and P. T. Cummings, *J. Chem. Phys.* **101**, 6206 (1994).
- [8] G. Marcelli, B. D. Todd, and R. J. Sadus, *Phys. Rev. E* **63**, 021204 (2001).
- [9] C. Desgranges and J. Delhommelle, *Phys. Rev. B* **78**, 184202 (2008).
- [10] S. N. Luo, T. J. Ahrens, T. Cagin, A. Strachan, W. A. Goddard, and D. C. Swift, *Phys. Rev. B* **68**, 134206 (2003).
- [11] P. Xu, T. Cagin, and W. A. Goddard, *J. Chem. Phys.* **123**, 104506 (2005).
- [12] C. Desgranges and J. Delhommelle, *J. Chem. Phys.* **128**, 084506 (2008).
- [13] K. P. Travis, P. J. Daivis, and D. J. Evans, *J. Chem. Phys.* **103**, 10638 (1995).
- [14] J. Delhommelle, J. Petracic, and D. J. Evans, *Phys. Rev. E* **68**, 031201 (2003).
- [15] J. Delhommelle, J. Petracic, and D. J. Evans, *J. Chem. Phys.* **119**, 11005 (2003).
- [16] J. Delhommelle, *Phys. Rev. E* **71**, 016705 (2005).
- [17] J. Delhommelle, *Phys. Rev. B* **69**, 144117 (2004).
- [18] J. Delhommelle and D. J. Evans, *Mol. Phys.* **99**, 1825 (2001).
- [19] J. Delhommelle and J. Petracic, *J. Chem. Phys.* **118**, 2783 (2003).
- [20] J. Delhommelle and D. J. Evans, *J. Chem. Phys.* **117**, 6016 (2002).
- [21] G. Pan, J. F. Ely, C. McCabe, and D. J. Isbister, *J. Chem. Phys.* **122**, 094114 (2005).
- [22] M. A. van der Hoef, *J. Chem. Phys.* **113**, 8142 (2000).
- [23] B. D. Todd, *Phys. Rev. E* **72**, 041204 (2005).